Published in final edited form as:
Proteins. 2011 April ; 79(4): 1267–1276. doi:10.1002/prot.22961.

Specificity and Cooperativity at β-lactamase Position 104 in TEM-1/BLIP and SHV-1/BLIP interactions

Melinda S. Hanes[1,2], **Kimberly A. Reynolds**[1,2,7], **Case McNamara**[3], **Partho Ghosh**[3], **Robert A. Bonomo**[4,5], **Jack F. Kirsch**[6], and **Tracy M. Handel**[2]

[1]Biophysics Graduate Group, University of California, Berkeley, Berkeley, CA 94729

[2]Skaggs School of Pharmacy and Pharmaceutical Sciences, University of California, San Diego, San Diego, CA 92093

[3]Department of Chemistry and Biochemistry, University of California, San Diego, San Diego, CA 92093

[4]Research Service, Louis Stokes Cleveland Department of Veterans Affairs Medical Center, Case Western Reserve University, Cleveland, Ohio, 44106

[5]Department of Pharmacology, Molecular Biology and Microbiology, Case Western Reserve University, Cleveland, Ohio, 44106

[6]Department of Molecular and Cell Biology, University of California, Berkeley, Berkeley, CA 94729

Abstract

Establishing a quantitative understanding of the determinants of affinity in protein-protein interactions remains challenging. For example, TEM-1/BLIP and SHV-1/BLIP are homologous β-lactamase/β-lactamase inhibitor protein complexes with disparate K_i values (3 nM and 2 μM, respectively), and a single substitution, D104E in SHV-1, results in a 1000-fold enhancement in binding affinity. In TEM-1, E104 participates in a salt bridge with BLIP K74, while the corresponding SHV-1 D104 does not in the wild type SHV-1/BLIP co-structure. Here, we present a 1.6 Å crystal structure of the SHV-1 D104E/BLIP complex that demonstrates that this point mutation restores this salt bridge. Additionally, mutation of a neighboring residue, BLIP E73M, results in salt bridge formation between SHV-1 D104 and BLIP K74 and a 400-fold increase in binding affinity. To understand how this salt bridge contributes to complex affinity, the cooperativity between the E/K or D/K salt bridge pair and a neighboring hot spot residue (BLIP F142) was investigated using double mutant cycle analyses in the background of the E73M mutation. We find that BLIP F142 cooperatively stabilizes both interactions, illustrating how a single mutation at a hot spot position can drive large perturbations in interface stability and specificity through a cooperative interaction network.

Keywords

cooperativity; double mutant cycle; BLIP; SHV-1; TEM-1; salt bridge; protein-protein interaction

Corresponding author: Tracy M. Handel University of California, San Diego Skaggs School of Pharmacy and Pharmaceutical Sciences 9500 Gilman Drive, MC 0684 La Jolla, CA 92093-0684 Phone: 858.822.6656 Fax: 858-822-6655 thandel@ucsd.edu.
[7]Present address, Department of Pharmacology, University of Texas Southwestern Medical Center, Dallas, TX 75390

Data Deposition:
The refined coordinates for the SHV-1 D104E/BLIP structure have been deposited in the Protein Data Bank (PDB ID **3N4I**).

Introduction

The experimentally well-characterized complex between TEM-1 β-lactamase and the β-Lactamase Inhibitor Protein (BLIP) has served as a useful model system for understanding protein-protein interactions. β-Lactamases catalyze the hydrolysis of the β-lactam moiety of drugs such as Penicillin G, which negates their pharmacological potency. BLIP, a potent inhibitor of a number of class A β-lactamases, is a 17.5 kDa protein isolated from the soil bacterium *Streptomyces clavuligerus*[1]. The best characterized partners of BLIP are TEM-1 and SHV-1, which recognize BLIP with a 1000-fold difference in inhibition constants (3 nM and 2 μM for TEM-1/BLIP and SHV-1/BLIP, respectively) even though the two enzymes share 67% amino acid identity and have nearly indistinguishable tertiary structures. The structural homology between SHV-1 and TEM-1 is maintained in the corresponding BLIP complexes – the aligned β-lactamases from the co-structures exhibit a C_α RMSD of 0.4 Å, and the associated BLIPs show a C_α RMSD of 1.0 Å[2]. BLIP competitively inhibits its β-lactamase targets by occluding the active site with two important binding loops: the F142 and D49 loops (Figure 1A). Both loops are named for the "hot-spot" residues they contain. The sidechains of BLIP F142 and D49 occupy similar positions as do the benzyl and carboxyl moieties of the substrate, Penicillin G.

The origins of specificity and affinity in the β-lactamase/BLIP system pose an interesting question. Several of BLIP's partners (TEM-1, SME-1, Bla1) share only ~30% identity, and yet they have similar affinity for BLIP, while SHV-1 and TEM-1, despite being more closely related with 67% identity, differ dramatically in their affinities for the inhibitor. Previously, we identified β-lactamase position 104, which is aspartate in SHV-1 and glutamate in TEM-1, as a key determinant of specificity[2]. The SHV-1 D104E mutation increases affinity for BLIP by a 1000-fold, resulting in a K_d value that is similar to that of TEM-1/BLIP. In the TEM-1/BLIP complex, E104 forms a salt bridge with BLIP K74 and makes van der Waals contacts with the BLIP F142 binding loop, whereas SHV-1 D104 does not show these interactions in the SHV-1/BLIP structure (Figure 1B). Furthermore, in a recent computational study employing the EGAD Library for protein design, a point mutation (BLIP E73M) was identified which resulted in a400-fold increase in affinity, due to the formation of a salt bridge between SHV-1 D104 and BLIP K74 (Figure 1B) [3].

Despite our previous success in designing SHV-1/BLIP complexes with enhanced affinity, accurately predicting the quantitative effects of mutations surrounding β-lactamase residue 104 has been challenging[3]. Mutations at several positions were outliers in the correlation between experimental and calculated ΔΔG values. For example, the impact of the mutations BLIP E73A, E73M, F142A, Y143A and SHV-1 D104A and D104E on complex affinity were underestimated[3]. Given that many design algorithms, including EGAD, are unable to model cooperative effects because of the use of pairwise decomposable energy functions to balance speed and accuracy, we hypothesized that cooperativity between these residues was the source of the computational mispredictions. Accordingly, in this study we experimentally investigated the cooperative interactions involving the β-lactamase 104/ BLIP K74 salt bridge and a neighboring residue (F142) in order to understand these non-trivial effects, and to provide data that may be used to improve existing computational algorithms.

Double mutant cycle (DMC) analysis is an experimental approach for inferring energetic interactions between sidechains by mutagenesis[4]. DMCs involve the characterization of the wild-type, two single, and the corresponding double mutations for a pair of residues in a protein or protein complex. For residues acting independently, $\Delta\Delta G_{mut}$ value for the double mutation is equal to the sum of $\Delta\Delta G_{mut}$ values for the individual mutations. However, if the effect of the mutation on a pair of residues deviates from the sum of individual mutational

effects, without any secondary effects (such as structural rearrangements), then the residue interactions are considered to be cooperative. The quantitative relationship, $\Delta\Delta G_{int}$, is given in equation 1.

$$\Delta\Delta G_{int} = \Delta\Delta G_{X\rightarrow A;Y\rightarrow B} - \Delta\Delta G_{X\rightarrow A} - \Delta\Delta G_{Y\rightarrow B} \quad \text{(Eq 1)}$$

Here, $\Delta\Delta G_{X\rightarrow A}$ and $\Delta\Delta G_{Y\rightarrow B}$ are the changes in free energy of dissociation upon mutation of residue X to A and Y to B, respectively; similarly $\Delta\Delta G_{X\rightarrow A;\ Y\rightarrow B}$ is the double mutation of X to A and Y to B. The coupling energy ($\Delta\Delta G_{int}$) generally decreases as the distance between residues increases; for example, in the barnase/barstar model system residues within 7 Å demonstrate cooperativity[5]. Nevertheless, there are reports documenting such effects between residues separated by as much as 25 Å, indicating that interactions are not always local[6,7].

Here, we report the 1.6 Å resolution crystallographic structure of the SHV-1 D104E/BLIP complex, which confirms the presence of the hypothesized salt bridge between the mutated E104 and BLIP K74 sidechains, and explains the 4.4 kcal/mol increase in affinity of the SHV-1 D104E complex with BLIP compared to wild type SHV-1. We also describe DMC analyses characterizing the E/K and D/K salt bridges in the TEM-1/BLIP E73M and SHV-1/BLIP E73M interfaces, with and without the proximal hot spot residue, BLIP F142. The results show that BLIP F142 stabilizes both salt bridges causing them to contribute favorably to binding affinity. However, the BLIP F142A mutation causes the salt bridge in the context of SHV-1/BLIP E73M to impact affinity negatively, and the salt bridge in TEM-1/BLIP E73M to have little effect on ΔG_{diss}, demonstrating the importance of coupled interactions in this interface.

Materials and Methods

Protein Expression and Purification

BLIP and SHV-1 were expressed and purified as previously described[2]. BLIP proteins requiring an additional purification step were further purified using a TEM-1-affinity column (NHS-Sepharose FF GE Healthcare). A pET-24a(+) based vector with an OmpA periplasmic signal sequence was used for TEM-1 expression. TEM-1 was expressed at 30°C by induction with isopropyl-B-$_D$-thiogalactopyranoside in *E. coli* BL21(DE3). Cells were harvested by centrifugation, and the periplasmic fraction isolated by osmotic shock followed by anion exchange chromatography (HiPrep 16/10 DEAE, GE Healthcare). Fractions containing TEM-1 were purified further by size exclusion chromatography (HiLoad 26/60 Superdex 75, GE Healthcare), and single-use aliquots of protein were stored at -80°C.

Crystallographic methods

Equimolar ratios of D104E SHV-1 and BLIP in 30mM BisTris, 50mM NaCl, pH 7.25, were concentrated to 5 mg/mL, and dialyzed overnight against the same buffer. Diffraction quality crystals were obtained by vapor diffusion (hanging drop format) at 18°C with 40 % ammonium sulfate (w/v) and 100 mM Tris (pH 8.5) as the crystallization condition. Trays were set by combining equal volumes (1 μL) of protein solution (5 mg/mL) and crystallization condition, above a 1 mL reservoir of crystallization condition. Crystals were added directly to the cryoprotectant solution (30% xylitol with crystallization condition), looped, and frozen in liquid nitrogen.

Datasets were collected at Beamline ID19 at the Advanced Photon Source (Argonne National Laboratory, Chicago). Diffraction data were scaled and integrated using HKL2000[8]; phasing was performed by molecular replacement with AMoRe using coordinates of the wild type SHV-1/BLIP structure (PDB ID 2G2U) as the initial model[9].

Iterations between manual rebuilding with O and refinement with REFMAC and ARP generated the final structural model[10-12]. Structural alignments and rmsd calculations were performed with LSQMAN[13]. Molecular figures were created with PyMOL[14].

Inhibition Assays

Dissociation constants for β-lactamase/BLIP complexes were determined by competition with the β-lactam substrate nitrocefin (Becton Dickinson Biosciences). Assays were performed with 2 nM enzyme in PBS (pH 7.4) with 0.1 mg/mL BSA at 26°C in quadruplicate in a 96-well plate format. The liquid handling capabilities of the FlexstationIII (Molecular Devices) initiated reactions by the addition of substrate, and absorbance at 486 nm was monitored.

Data was normalized to the observed activity without the inhibitor (fractional activity). IC_{50} values were obtained by plotting fractional activity versus total inhibitor concentration, and fitting to Morrison's equation (Eq 2) with OriginPro.

$$f_{activity} = 1 - \frac{[E_0] + [I_0] + IC_{50} - \sqrt{\{[E_0] + [I_0] + IC_{50}\}^2 - 4[E_0][I_0]}}{2[E_0]} \quad \text{Eq (2)}$$

Dissociation constants were calculated from the IC_{50} value by applying the Cheng-Prusoff correction (Eq 3) [15].

$$K_d = \frac{IC_{50}}{1 + [S]/K_m)} \quad \text{Eq (3)}$$

The K_m value of the enzyme for the β-lactam substrate, nitrocefin, was determined in a separate experiment, and fit to the Michaelis-Menton equation using OriginPro.

Results

SHV-1 D104E/BLIP: A salt bridge between β-lactamase position 104 and BLIP K74 increases affinity

β-Lactamase position 104 has been described as a specificity determinant in the β-lactamase/BLIP interface due to the observation that the SHV-1 D104E mutation increases the binding energy to BLIP by 4.4 kcal/mol[2]. In this work, the inverse TEM-1 E104D mutation was characterized in TEM-1. As predicted, this mutant displays micromolar affinity for BLIP, which is similar to that of wild-type SHV-1, further confirming its role as a specificity determinant (Table 1). Furthermore, TEM-1 and SHV-1 have similar dissociation constants for the BLIP complex when the same amino acid (Ala, Asp, Glu, or Lys) is placed at β-lactamase position 104.

The SHV-1 D104E mutation was hypothesized to facilitate the formation of an intermolecular salt bridge between SHV-1 E104 and BLIP K74, as observed in the native TEM-1/BLIP co-structure. To determine the interactions responsible for enhanced affinity in the SHV-1 D104E point mutant, the co-structure was solved to 1.6 Å resolution by crystallography (Table 2). As predicted, the carboxyl oxygen of SHV-1 E104 (Oε2) makes an intermolecular hydrogen bond with the amine nitrogen of BLIP K74 (Nζ) (Oε2-Nζ distance = 3.0 Å), and with BLIP backbone amide of Y143 (Oε2-N distance = 2.9 Å), mimicking the TEM-1/BLIP native interactions (Figure 2A-B). The SHV-1 D104E /BLIP structure is highly similar to that of the wild type complex, with a C_α RMSD of 0.2 Å (430

atoms compared). Restricting the alignment to residues within 5 Å of either salt bridging partner yields an RMSD of 0.4 Å (255 atoms compared) for all non-hydrogen atoms between the D104E mutant complex and wild type SHV-1/BLIP. Hence, the D104E mutation does not significantly perturb local sidechain conformations or induce backbone rearrangements, and the increase in affinity can be attributed to E104 interactions. Due to the larger volume of glutamate versus aspartate, van der Waals contacts across the interface with BLIP F142 and Y143 are observed. In addition to contributing new, favorable interactions, the SHV-1 D104E mutation also relieves an electrostatic clash between wild type SHV-1 D104 and BLIP E73. The unfavorable interaction between these two sidechains was previously proposed to explain the BLIP alanine mutagenesis results for SHV-1[16]. The extra methylene group of glutamate with respect to aspartate increases the distance between the proximal carboxyl group atoms, from 5.5 Å in wild type, to 6.0 Å in the mutant structure.

It was recently reported that the BLIP mutation E73M allows SHV-1 D104 to assume a conformation suitable for salt bridging with BLIP K74 by removing the carboxyl group at position E73 (Figure 1B) [2]. The K_i value for the SHV-1/BLIP E73M complex is ~1 nM. In the context of BLIP E73M, we performed double mutant cycle analysis of the salt bridge between β-lactamase position 104 and BLIP K74 for both the SHV-1/BLIP and the TEM-1/BLIP complexes. For clarity and concision, β-lactamase/BLIP complexes containing the E73M BLIP mutation are referred to as BLIPM (for example, TEM-1/BLIPM and SHV-1/BLIPM). This BLIPM background eliminates the contributions from the unfavorable interaction between BLIP E73 and SHV-1 D104. The influence of a proximal hydrophobic residue and hot spot, BLIP F142, was also investigated.

BLIP F142 cooperatively stabilizes the Glu/Lys and Asp/Lys salt bridges

The introduction of the double alanine D/K or E/K salt bridge mutations causes a reduction in ΔG_{diss} of 0.9 kcal/mol and 1.6 kcal/mol in the SHV-1/BLIPM and TEM-1/BLIPM complexes, respectively (Table 3). By contrast, the single β-lactamase D104A or E104A mutations (referred to as X104A) result in $\Delta\Delta G_{diss}$ values of 0.3 and 1.3 kcal/mol for the SHV-1/BLIPM and TEM-1/BLIPM complexes, respectively (Table 3). BLIP K74A is more destabilizing to both interfaces than are the corresponding β-lactamase X104A mutations, with $\Delta\Delta G_{diss}$ values of 2.9 and 3.8 kcal/mol for SHV-1 and TEM-1, respectively. To investigate the electrostatic potential in the interface, the surface map was calculated using Adaptive Poisson-Boltzman Solver (APBS) and the results were visualized in PyMOL[14,17] (Figure 3). The SHV-1/BLIP complex has substantial negative electrostatic potential in the BLIP interface (Figure 3A) that is enhanced in the case of BLIP K74A (Figure 3B), and partially neutralized by the SHV-1 D104A mutation (Figure 3C).

Double mutant cycle results and coupling energies indicate cooperativity

Extension of DMC analysis to groups of more than two residues yields useful information about cooperativity. Three interacting residues can be systematically mutated in two double mutant cycles, or a cubic cycle (depicted in Figure 4)[18]. Each vertex represents a different mutant complex, while a single mutation differentiates two connected edges, and the corresponding $\Delta\Delta G$ value is given along the edge. The bottom face of each cube differs from the top cycle by the addition of the BLIP F142A mutation. This depiction illustrates the stabilizing effect (or lack of such in the mutant) of F142 on the salt bridge pair. The extent to which the top and bottom cycles differ describes the dependence of the interaction on a third residue, or the coupling energy.

BLIP F142A differentially affects the free energies of dissociation in the SHV-1 D104/BLIPM K74 and TEM-1 E104/BLIPM K74 complexes (Figure 4). In the background of

BLIPM F142A, the D/K salt bridge does not appear to enhance the affinity of SHV-1 for BLIPM; in fact, the double alanine mutation is more favorable by 1.3 kcal/mol. In the TEM-1 interface, the ion pair is energetically neutral in the presence of BLIPM F142A ($\Delta\Delta G_{diss}$ = 0.1 kcal/mol).

Significant coupling energies are observed between most residue pairs investigated (Table 4). The largest was found between the oppositely charged salt bridging residues, followed closely by the coupling of BLIP K74 and the neighbor aromatic BLIP F142. In general, coupling energy uncertainty is 0.3 kcal/mol, which is in the range of previous studies[5,19,20]. Another schematic representation of the data is a plot of additive versus experimental $\Delta\Delta G_{diss}$ values for pairs of mutated residues (Figure 5). Data points for completely additive or independent residues would lie on a line with unit slope that intercepts the origin. Most pairs of residues that were probed within the TEM-1/BLIPM and SHV-1/BLIPM interfaces demonstrate anti-cooperativity, or positive coupling, indicating that the simultaneous replacement of both residues is more deleterious than both single replacements.

Discussion

Consequences of β-lactamase 104 and BLIP K74 mutations

Earlier explanations for the change in BLIP affinity caused by β-lactamase 104 variants focused on the TEM-1 E104 and BLIP K74 putative salt bridge[2]. It was suggested that because of the smaller side chain of D104, SHV-1 D104 can not form a TEM-like salt bridge with BLIP K74. Additionally, the larger volume of E104 in TEM-1 was proposed to make favorable van der Waals contacts with the BLIP F142 loop, thus stabilizing its position in the interface. Furthermore, the stabilities of TEM-1/BLIP and SHV-1/BLIP complexes are similar when the β-lactamase contains the same residue at position 104.

These results would argue that the glutamate-to-aspartate substitution is the sole contributor to the thousand-fold difference in dissociation constants of the wild type complexes. However, there are seven additional amino acids differences between the SHV-1/BLIP and TEM-1/BLIP interfaces that have not been characterized in the context of the alternate β-lactamase/BLIP interface. Five conservative mutations (Q100N, D104E, S133T, R215K, and T235S) and three non-conservative substitutions (R98S, A114T, T167P) differentiate the SHV-1/BLIP from the TEM-1/BLIP interface. Inspection of the crystallographic structures suggested that in some cases the native TEM-1 sidechain results in more favorable interactions with BLIP, while in other cases the wild type SHV-1 residue may be optimal[2].

While all combinations of substitutions distinguishing the two β-lactamases have not been characterized, the importance of the D104E substitution can be quantitatively evaluated via Eqs 4 and 5[21,22].

$$I = \Delta\Delta G_{A_{X\to Y}} - \Delta\Delta G_{B_{Y\to X}} \quad \text{(Eq 4)}$$

$$C = \Delta\Delta G_{A_{X\to Y}} + \Delta\Delta G_{B_{Y\to X}} \quad \text{(Eq 5)}$$

The impact (I) and context dependence (C) of a position is the difference and sum, respectively, of the $\Delta\Delta G_{diss}$ values for forward and reverse replacements in a pair of homologous proteins, A and B, which contain residue X or Y at a single site. Here, $\Delta\Delta G_{A X\to Y}$ is the free energy of dissociation difference between the X-to-Y mutant and wild type for protein A; and $\Delta\Delta G_{B Y\to X}$ refers to the corresponding quantity for the inverse mutation, Y-to-X, and wild type for protein B. This analysis when applied to the β-lactamase/BLIP X104 exchange mutations (SHV-1 D104E/BLIP and TEM-1 E104D/BLIP),

yields *I* and *C* values of -8.0 ± 0.4 kcal/mol and -0.8 ± 0.4 kcal/mol, respectively. Thus, the significant *I* value proves that the position is important, and the small *C* value indicates that the mutation is nearly context independent. Of note, the I/C analysis refers to β-lactamase mutants interacting with wild type BLIP, and does not include cooperativity with BLIP F142. The almost context independence is expected, because only one other amino difference (P167T in TEM-1) is present within 10 Å of position 104.

On the opposite side of the interface, the BLIP K74A mutation is more destabilizing than either β-lactamase X104A, or the double alanine mutation. While the β-lactamase X104A mutation removes the salt bridge, it has the favorable effect of increasing the electrostatic complementarity at the interface (Figure 3). Additionally, the change in sidechain volume associated with the lysine-to-alanine mutation is more significant than that associated with the corresponding aspartate-to-alanine mutation. Although alanine mutations are most often utilized to dissect the importance of salt bridges, when the ion pairs are considered alongside their hydrophobic isosteres, enhanced affinity is not necessarily observed[23]. Therefore, the $\Delta\Delta G_{diss}$ for the more isosteric lysine-to-methionine mutation may be less significant than the value for the lysine-to-alanine substitution.

BLIP F142 may orient and shield the participating ion pairs from bulk solvent

The center of mass of BLIP F142 is 4.1 Å from TEM-1 E104 Oε1 and 5.6 Å from BLIP K74 Nζ. Thus, due to proximity, BLIP F142 may influence the local environments of the E/K and D/K salt bridges, thereby contributing to a cooperative network. In the TEM-1/BLIPM context, the salt bridge contributes 1.6 kcal/mol to the total binding energy, and is neutral in the case of BLIP F142A. In the SHV-1/BLIPM complex, the D/K pair contributes 0.9 kcal/mol, while in the F142A mutant, the pair oppose binding. The results indicate that F142A weakens the salt bridge interaction in the TEM-1/BLIPM interface, and removes it entirely in the SHV-1/BLIPM interface. We hypothesize that BLIP F142 may strengthen the salt bridge by optimally orienting the participating atoms and/or by shielding them from solvent, similar to what has been proposed for the Tyr434 hot spot in the hRI/RNase A interface[24]. In order to test this theory we attempted to characterize additional BLIP F142 mutants, however the mutation (BLIP F142W) resulted in poor expression and yield.

BLIP F142A destabilizes the SHV-1 complex more than the TEM-1 complex. Although BLIP F142 makes favorable van der Waals contacts in both interfaces, an additional intermolecular interaction is present only in the TEM-1 complex: TEM-1 E104 Oε1 maintains a hydrogen bond to BLIP Y143 N, while the corresponding D104 in the SHV-1/BLIP interface does not (Figure 6A). Therefore, in the SHV-1 interface, it is possible that F142A may destabilize the BLIP F142 binding loop, perhaps enough to displace its original position from the interface. In fact, the F142 loop is observed in alternate conformations in several mutant complexes, including SHV-1/BLIP D104K, TEM-1 E104Y Y105N/BLIP, as well as the homologous KPC-2/BLIP complex[2,25,26].

The crystallographic structure of the TEM-1/BLIP F142A complex, presented by Schreiber and co-workers, reveals an unraveling of local sidechain interactions as a result of the mutation[27]. In the TEM-1/BLIP F142A co-structure, TEM-1 E104 adopts an alternate rotamer, which increases the distance between the E/K donor-acceptor pair from 2.7 Å, a normal hydrogen bonding distance, to 4.5 Å in the mutant, which is too long for hydrogen bond formation (Figure 6B). By extending these structural findings to the TEM-1/BLIPM F142A complex, we suggest that BLIP F142 exerts its cooperative effect on the salt bridge partly by affecting the geometry of the hydrogen bond pair. Additionally, it has been reported that the aspartate and glutamate residues present in solvated protein interfaces preferentially hydrogen bond to buried water instead of forming salt bridges[28]. Consistent with these observations, are the results from the DMC analysis that show that the wild-type

salt bridge contributes favorably to binding, while the same interaction in the context of the BLIP F142A mutant complex has a negligible effect.

The cooperativity of salt bridge networks has been described in the TEM-1/BLIP system[19]. Albeck *et al.* suggested that salt bridges existing in networks contribute favorably to affinity, but in isolation they may contribute neutrally or negatively. Similarly, here we described the cooperative effect of a neighboring hydrophobic residue on a salt bridging pair, further demonstrating the environmental dependence of such interactions. Li and Liang find that two oppositely charged residues are more commonly found in proximity to an aromatic residue than is expected from the pairwise probabilities in protein cores and less often than expected on protein surfaces[29]. This may suggest that the example presented here, the modulation of a salt bridge by a nearby residue, is a commonly utilized motif in protein-protein interactions.

Cooperativity in hot spots and implications for protein design

The work presented here illustrates how cooperative interactions at a hot spot drive interface specificity between two homologous protein complexes. Additionally, the BLIP F142A mutation demonstrates that a single mutation can significantly alter the energetic contribution of a number of residues through a cooperative network. Despite the fact that cooperativity is a hallmark of natural proteins, computational methods have thus far proven inadequate for quantitatively capturing cooperative effects. A decade ago it was suggested that indirect effects were responsible for the difficulty in computationally predicting the effect of mutations[30]. Hence, new algorithms (that do not rely solely on pairwise interactions) need to be developed to increase our accuracy in predicting cooperative effects for protein design applications. The thermodynamic and structural data presented here not only increase our understanding of cooperative effects, but also provide a useful example and test case for the development of such methodology.

Acknowledgments

T.M.H. gratefully acknowledges support from NSF grant 0344749. K.A.R was supported by a NSF graduate research fellowship. R.A.B. would like to acknowledge the U.S. Department of Veterans Affairs Merit Review Program, VISN 10 GRECC, and National Institutes of Health (NIH) grant 1R01 A1063517-01 for support. J.F.K was supported by NIGMS (GM35393).

Abbreviations and symbols

BLIP	β-lactamase inhibitor protein
DMC	double mutant cycle

References

1. Strynadka N, Jensen S, Johns K, Blanchard H, Page M, Matagne A, Frère J, James M. Structural and kinetic characterization of a β-lactamase inhibitor protein. Nature. 1994; 368(6472):657–660. [PubMed: 8145854]
2. Reynolds KA, Thomson JM, Corbett KD, Bethel CR, Berger JM, Kirsch JF, Bonomo RA, Handel TM. Structural and computational characterization of the SHV-1 β-lactamase/β-lactamaseinhibitor proteininterface. J Biol Chem. 2006; 281(36):26745–26753. [PubMed: 16809340]
3. Reynolds KA, Hanes MS, Thomson JM, Antczak AJ, Berger JM, Bonomo RA, Kirsch JF, Handel TM. Computational redesign of the SHV-1 β-lactamase-β-lactamase inhibitor protein interface. J Mol Biol. 2008; 382(5):1265–1275. [PubMed: 18775544]

4. Carter PJ, Winter G, Wilkinson AJ, Fersht AR. The use of double mutants to detect structural changes in the active site of the tyrosyl-tRNA synthetase (*Bacillus stearothermophilus*). Cell. 1984; 38(3):835–840. [PubMed: 6488318]
5. Schreiber G, Fersht AR. Energetics of protein-protein interactions: Analysis ofthe barnase-barstar interface by single mutations and double mutant cycles. J Mol Biol. 1995; 248(2):478–486. [PubMed: 7739054]
6. Moza B, Buonpane R, Zhu P, Herfst C, Rahman A, McCormick J, Kranz D, Sundberg E. Long-range cooperative binding effects in a T cell receptor variable domain. Proc Natl Acad Sci USA. 2006; 103(26):9867–9872. [PubMed: 16788072]
7. Wang J, Palzkill T, Chow D-C. Structural insight into the kinetics and ΔCp of interactions between TEM-1 β-lactamase and β-lactamase inhibitory protein (BLIP). J Biol Chem. 2009; 284(1):595–609. [PubMed: 18840610]
8. Otwinowski, Z.; Minor, W. Processing of X-ray diffraction data collected in oscillation mode.. In: Carter, CWJ.; Sweet, RM., editors. Methods in Enzymology. Vol. 276. Academic Press; New York: 1997. p. 307-326.
9. Navaza J. AMoRe: an automated package for molecular replacement. Acta Cryst A. 1994; 50(2): 157–163.
10. Vagin AA, Steiner RA, Lebedev AA, Potterton L, McNicholas S, Long F, Murshudov GN. REFMAC5 dictionary: organization of prior chemical knowledge and guidelines for its use. Acta Cryst D. 2004; 60(12 Part 1):2184–2195. [PubMed: 15572771]
11. Jones, TA.; Kjeldgaard, MO. The Manual, Version 7.0. Uppsala Software Factory; Uppsala, Sweden: 1997.
12. Collaborative-Computational-Project. “The CCP4 suite: programs for protein crystallography”. Acta Cryst. 1994; D50:750–763.
13. Kleywegt G. Use of non-crystallographic symmetry in protein structure refinement. Acta Cryst D. 1996; 52(4):842–857. [PubMed: 15299650]
14. DeLano, WL. The PyMOL molecular graphics system. DeLano Scientific; Palo Alto, CA, USA: 2002. http://www.pymol.org
15. Cheng Y-C, Prusoff WH. Relationship between the inhibition constant (KI) and the concentration of inhibitor which causes 50 per cent inhibition (I50) of an enzymatic reaction. Biochem Pharmacol. 1973; 22(23):3099–3108. [PubMed: 4202581]
16. Zhang Z, Palzkill T. Dissecting the protein-protein interface between β-lactamase inhibitory protein and class A β-lactamases. J Biol Chem. 2004; 279(41):42860–42866. [PubMed: 15284234]
17. Baker NA, Sept D, Joseph S, Holst MJ, McCammon JA. Electrostatics of nanosystems: Application to microtubules and the ribosome. Proc Natl Acad Sci USA. 2001; 98(18):10037–10041. [PubMed: 11517324]
18. Horovitz A, Serrano L, Avron B, Bycroft M, Fersht AR. Strength and co-operativity of contributions of surface salt bridges to protein stability. Journal of Molecular Biology. 1990; 216(4):1031–1044. [PubMed: 2266554]
19. Albeck S, Unger R, Schreiber G. Evaluation of direct and cooperative contributions towards the strength of buried hydrogen bonds and salt bridges. J Mol Biol. 2000; 298(3):503–520. [PubMed: 10772866]
20. Harel M, Cohen M, Schreiber G. On the dynamic nature of the transition state for protein-protein association as determined by double-mutant cycle analysis and simulation. J Mol Biol. 2007; 371(1):180–196. [PubMed: 17561113]
21. Luong TN, Kirsch JF. A general method for the quantitative analysis of functional chimeras: Applications from site-directed mutagenesis and macromolecular association. Protein Science. 2001; 10(3):581–591. [PubMed: 11344326]
22. Chow MA, McElroy KE, Corbett KD, Berger JM, Kirsch JF. Narrowing Substrate Specificity in a Directly Evolved Enzyme: The A293D Mutant of Aspartate Aminotransferase. Biochem. 2004; 43(40):12780–12787. [PubMed: 15461450]

23. Pons J, Rajpal A, Kirsch JF. Energetic analysis of an antigen/antibody interface: Alanine scanning mutagenesis and double mutant cycles on the hyhel-10/lysozyme interaction. Protein Sci. 1999; 8(5):958–968. [PubMed: 10338006]

24. Chen C-Z, Shapiro R. Superadditive and subadditive effects of “Hot Spot” mutations within the interfaces of placental ribonuclease inhibitor with angiogenin and ribonuclease A. Biochem. 1999; 38(29):9273–9285. [PubMed: 10413501]

25. Hanes MS, Jude KM, Berger JM, Bonomo RA, Handel TM. Structural and biochemical characterization of the interaction between KPC-2 β-lactamase and β-lactamase inhibitor protein. Biochemistry. 2009; 48(39):9185–9193. [PubMed: 19731932]

26. Reichmann D, Cohen M, Abramovich R, Dym O, Lim D, Strynadka NCJ, Schreiber G. Binding hot spots in the TEM1-BLIP interface in light of its modular architecture. J Mol Biol. 2007; 365(3):663–679. [PubMed: 17070843]

27. Reichmann D, Rahat O, Albeck S, Meged R, Dym O, Schreiber G. The modular architecture of protein-protein binding interfaces. Proc Natl Acad Sci USA. 2005; 102(1):57–62. [PubMed: 15618400]

28. Bueno M, Camacho C,J. Acidic groups docked to well defined wetted pockets at the core of the binding interface: A tale of scoring and missing protein interactions in CAPRI. Proteins. 2007; 69(4):786–792. [PubMed: 17803211]

29. Li X, Liang J. Geometric cooperativity and anticooperativity of three-body interactions in native proteins. Proteins. 2005; 60(1):46–65. [PubMed: 15849756]

30. Shapiro R, Ruiz-Gutierrez M, Chen C-Z. Analysis of the interactions of human ribonuclease inhibitor with angiogenin and ribonuclease A by mutagenesis: importance of inhibitor residues inside versus outside the C-terminal “hot spot”. J Mol Biol. 2000; 302(2):497–519. [PubMed: 10970748]

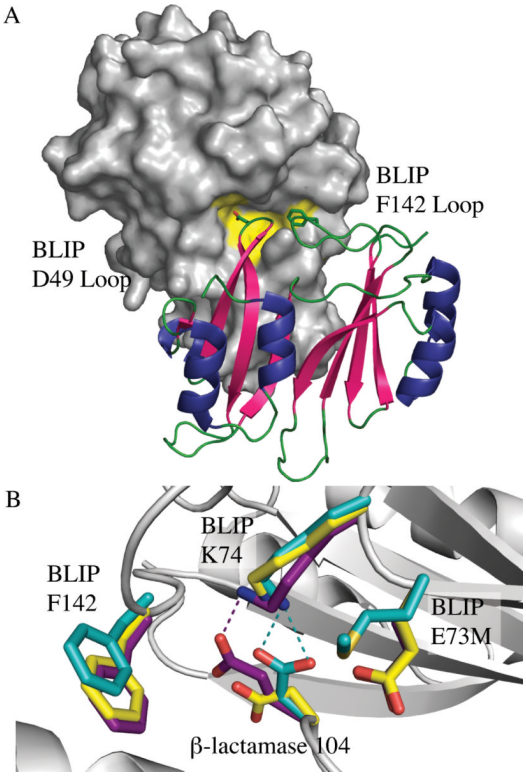

Figure 1.
The SHV-1/BLIP interface (PDB ID 2G2U). *A)* BLIP occludes the active site (yellow) of SHV-1 (gray surface) with the D49 and F142 binding loops. B) In the TEM-1/BLIP interface (purple, PDB ID 1JTG), TEM-1 E104 participates in a salt bridge (purple dash) with BLIP K74, while the corresponding SHV-1 D104 sidechain does not (yellow). However, in the SHV-1/BLIP E73M interface (cyan, PDB ID 3C4P), a salt bridge (cyan dash) is formed between SHV-1 D104 and BLIP K74.

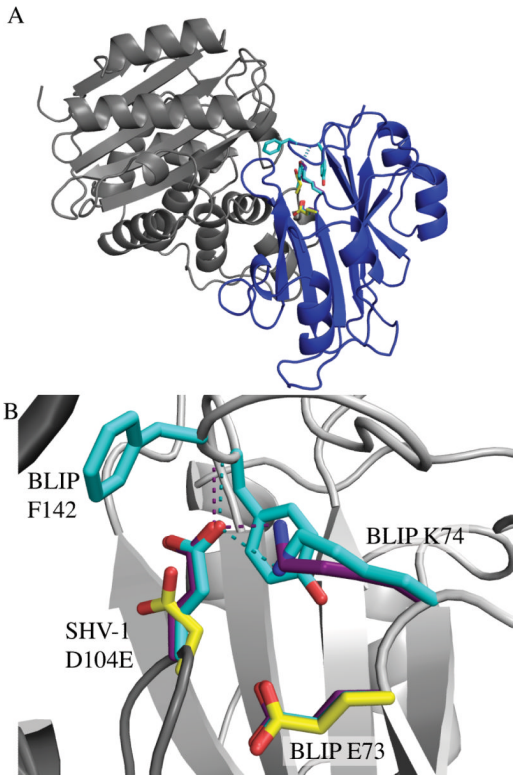

Figure 2.
The 1.6 Å resolution crystallographic structure of the SHV-1 D104E/BLIP complex reveals the interactions responsible for the enhanced affinity (PDB ID 3N4I). *A)* SHV-1 D104E (gray) bound to BLIP (blue). *B)* In the SHV-1 D104E/BLIP structure (cyan), E104 participates in a salt bridge (cyan dash) with BLIP K74, similar to that observed in the wild type TEM-1/BLIP structure (purple, PDB ID 1JTG). Residues from the wild type SHV-1/BLIP co-structure (yellow, PDB ID 2G2U) are shown for comparison.

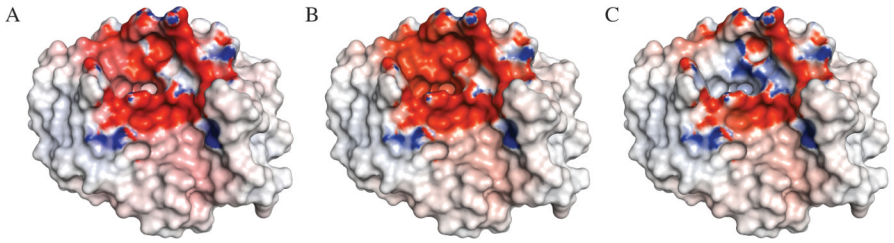

Figure 3.

The surface of BLIP colored by residual electrostatic potential in the SHV-1/BLIP complex for the mutants assayed in the double mutant cycle procedure (PDB ID 2G2U): *A)* the BLIP surface from SHV-1/BLIP E73M; *B)* the BLIP surface from SHV-1/BLIP E73M/K74A; *C)* the BLIP surface from SHV-1 D104A/BLIP E73M. Figures were prepared with PyMOL and APBS using an ionic strength of 0.15 M, and protein and solvent dielectric constants of 2 and 80, respectively. The colorimetric scale shown is from 0 to -20 kT/*e* potential in red and 0 to 20 kT/*e* potential in blue.

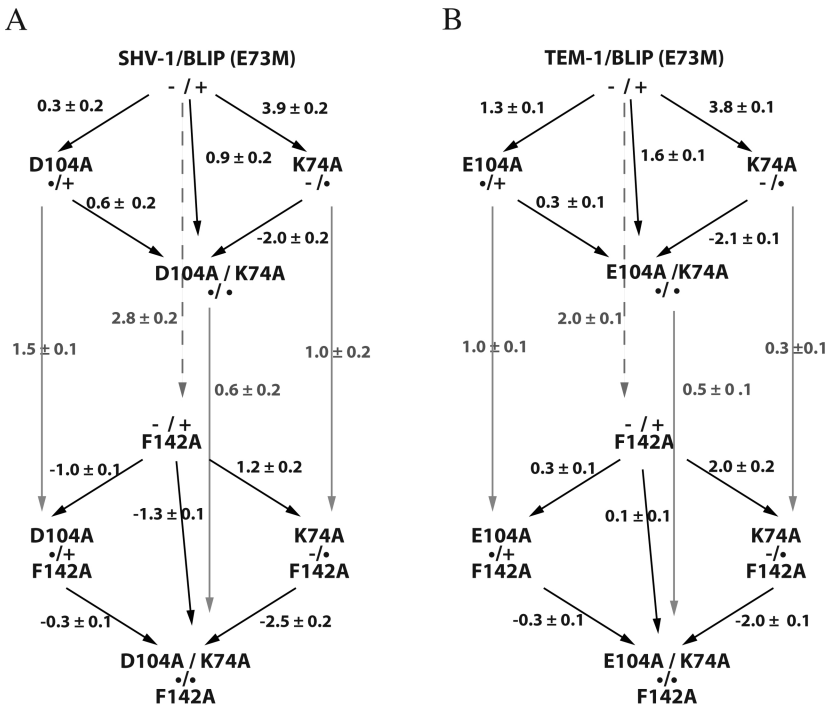

Figure 4.

Double mutant cycle analysis of the salt bridge between β-lactamase X104 and BLIP K74, in the BLIP E73M context. Each vertex represents a different mutant and the $\Delta\Delta G_{diss}$ values between mutants are given along each edge. Symbols indicate the presence (+ or -) or absence (•) of a charged residue type. The lower plane of each cube differs from the upper plane by the BLIP F142A mutation. *A)* The SHV-1/BLIP and *B)* the TEM-1/BLIP double mutant cycle analyses.

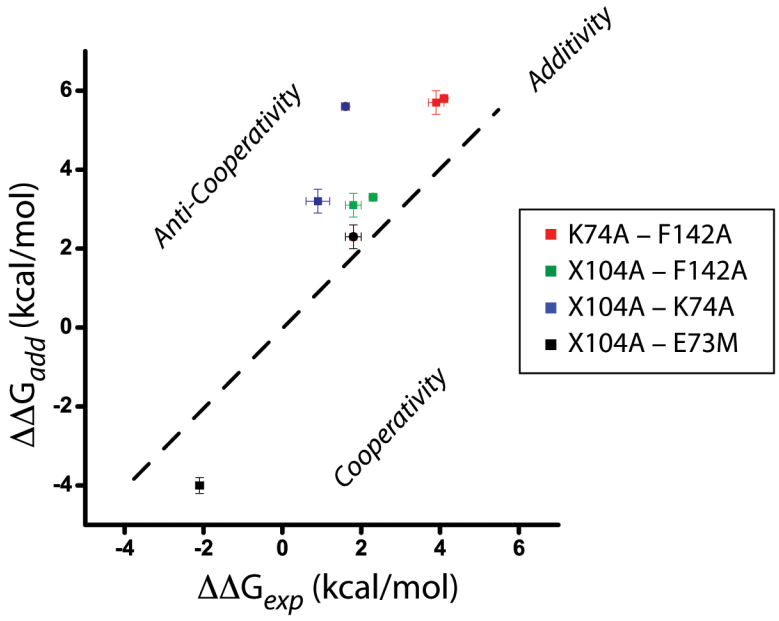

Figure 5.

Additive versus experimental ΔΔG values for pairs of mutated residues. Completely additive or independent residues yield a line with slope of unity and intercepting the origin (dashed line). Each point represents a pair of residues probed in single and the corresponding double alanine mutation for either the TEM-1/BLIP and SHV-1/BLIP interfaces colored by mutations. Most pairs of residues investigated demonstrate anti-cooperativity.

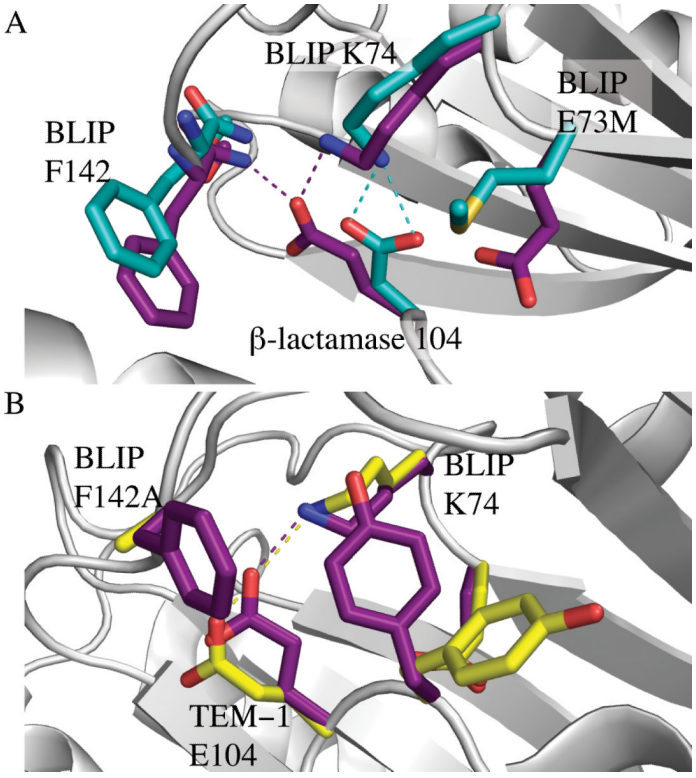

Figure 6.

BLIP F142 modulates the strength of the β-lactamase 104/BLIP K74 salt bridge. *A)* In the TEM-1/BLIP interface (purple, PDB ID 1JTG), TEM-1 E104 makes a hydrogen bond with the backbone amide of the BLIP F142 loop while the corresponding D104 from the SHV-1/BLIP E73M interface (cyan, PDB ID 3C4P) does not. *B)* The TEM-1/BLIP F142A crystallographic structure (yellow, PDB ID 1SOW) shows non-hydrogen bonding conformations for TEM-1 E104 and BLIP K74, in addition to an alternate conformation for the neighboring TEM-1 Y105 sidechain. Wild-type conformations are shown for comparison (purple).

Table 1

Dissociation constants for β-lactamase/BLIP mutant complexes. Values for the wild type complex are in bold.

β-lactamase mutation	SHV-1/BLIP K_d (nM)	$\Delta\Delta G_{mut}$ (kcal/mol)	TEM-1/BLIP K_d (nM)	$\Delta\Delta G_{mut}$ (kcal/mol)
104-Ala	133 ± 7	-1.5 ± 0.1	70 ± 5	1.8 ± 0.2
104-Asp	**1800 ± 100**	–	1500 ± 100	3.6 ± 0.2
104-Glu	1.1 ± 0.2	-4.4 ± 0.3	**3.2 ± 0.4**	–
104-Lys[a]	580 ± 40	-0.7 ± 0.1	140 ± 5	2.2 ± 0.2

[a]Values from ref 11.

Table 2

Crystallographic data collection, refinement and stereochemistry parameters for the SHV-1 D104E / BLIP structure.

SHV-1 D104E/BLIP (PDB ID 3N4I)	
Data Collection	
Resolution (Å)	1.56 - 110
Wavelength (Å)	1.1159
Space Group	P 6_3
Unit Cell Dimensions	127.9, 127.9, 73.2
Unit Cell Angles (α,β,γ)°	90.0, 90.0, 120.0
I/σ (last shell)	17.9 (3.0)
R_{sym} (last shell) %	8.2 (44.7)
Completeness (last shell)	99.6 (96.8)
No. of reflections	187424
unique	96515
Refinement	
Resolution (Å)	1.56 -110
No. of reflections	91252
working	86611
free (% total)	4641 (5.1)
R_{work} (last shell) (%)	17.0 (26.2)
R_{free} (last shell) (%)	17.9 (27.8)
Structure and Stereochemistry	
No. of atoms	3625
protein	3260
water	365
RMSD bond lengths (Å)	0.010
RMSD bond angles (°)	1.305
Ave B	20.9

$R_{sym} = \Sigma\Sigma_j|I_j - \langle I\rangle|\Sigma I_j$, where I_j is the intensity measurement for reflection j, and $\langle I\rangle$ is the mean intensity for multiple recorded reflections. $R_{work,free} = \Sigma||F_o| - |F_c||F_o|$, where the working and free R-factors are calculated using the working and free reflection sets, respectively. The free reflections were held aside throughout the refinement.

Table 3

Dissociation constants for TEM-1/BLIP and SHV-1/BLIP mutant complexes constituting the double mutant cycle analyses.

	SHV-1		SHV-1 D104A	
BLIP mutant	**K_i (nM)**	**ΔΔG (E73M)**	**K_i (nM)**	**ΔΔG (E73M)**
WT	**1800 ± 100**	2.5 ± 0.2	133 ± 7	0.9 ± 0.2
E73M	28 ± 3	-	48 ± 4	0.3 ± 0.2
E73M/K74A	4000 ± 300	2.9 ± 0.2	130 ± 20	0.9 ± 0.3
E73M/F142A	3100 ± 200	2.8 ± 0.2	560 ± 40	1.8 ± 0.2
E73M/K74A/F142A	22000 ± 3000	3.9 ± 0.2	340 ± 20	1.5 ± 0.2

	TEM-1		TEM-1 E104A	
	K_i (nM)	**ΔΔG (E73M)**	**K_i (nM)**	**ΔΔG (E73M)**
WT	**3.2 ± 0.4**	-0.5 ± 0.2	70 ± 5	1.3 ± 0.1
E73M	7.5 ± 0.4	-	71 ± 2	1.3 ± 0.1
E73M/K74A	4500 ± 400	3.8 ± 0.1	110 ± 5	1.6 ± 0.1
E73M/F142A	230 ± 10	2.0 ± 0.1	390 ± 20	2.3 ± 0.1
E73M/K74A/F142A	7000 ± 400	4.1 ± 0.1	250 ± 7	2.1 ± 0.1

Table 4

Free energies of interaction for SHV-1/BLIP and TEM-1/BLIP residues were calculated according to equation 1.

BLIP Mutation	SHV-1 complex	$\Delta\Delta G_{int}$	TEM-1 complex	$\Delta\Delta G_{int}$
E73M	D104A	1.9 ± 0.2	E104A	-0.5 ± 0.3
K74A	F142A	-1.8 ± 0.3	F142A	-1.7 ± 0.2
F142A	D104A	-1.3 ± 0.3	E104A	-1.0 ± 0.2
K74A	D104A	-2.3 ± 0.4	E104A	-4.0 ± 0.2